



TESTS OF SCALED PILE CAPS PART 1: SIZE EFFECT

L. Laughery⁽¹⁾, T. Ichinose⁽²⁾, K. Kasai⁽³⁾, K-Y. Liu⁽⁴⁾, S. Komatsu⁽⁵⁾,
K-Y. Liu⁽⁶⁾, Y. Nakagami⁽⁷⁾, T. Matsunoshita⁽⁸⁾

⁽¹⁾ Associate, Exponent, llaughery@exponent.com

⁽²⁾ Professor, Nagoya Institute of Technology, ich@nitech.ac.jp

⁽³⁾ Professor, Tokyo Institute of Technology, kasai.k.ac@m.titech.ac.jp

⁽⁴⁾ Associate Professor, National Cheng Kung University, kyluu@gs.ncku.edu.tw

⁽⁵⁾ Assistant Professor, Shimane University, s.komatsu@riko.shimane-u.ac.jp

⁽⁶⁾ Graduate Student, National Cheng Kung University, ckck89105@gmail.com

⁽⁷⁾ Graduate Student, Nagoya Institute of Technology, yohhen031@gmail.com

⁽⁸⁾ Undergraduate Student, Nagoya Institute of Technology, nknlturjn@gmail.com

Abstract

Super-tall buildings are being constructed all around the world. With element sizes larger than what has been tested in the laboratory and what has been built before, these buildings are pushing the boundaries of our engineering experience. But with increase in size comes questions about whether the strength and behavior of super-sized structural elements can be estimated using current methods and experience. In reinforced concrete elements loaded in one-way shear, past investigations have noted a reduction in concrete unit shear strength with increasing member size. Dubbed the “size effect,” this phenomenon was recently incorporated into the American Concrete Institute’s Building Code Requirements for Structural Concrete (ACI 318-19). Questions remain about whether there is such an effect for reinforced concrete elements loaded in two-way shear. And as buildings become larger and foundations deepen as a result, it is critical to determine whether pile caps loaded in two-way shear may exhibit a similar size effect. To investigate this phenomenon, twelve pile cap specimens were tested to failure under uniaxial compression. Both heavily-reinforced specimens and lightly-reinforced specimens were constructed at each scale. This paper discusses results of heavily-reinforced specimens failing in shear at small steel strains. The results showed a reduction in unit strength when effective depth increased from 250mm to 1000mm. The results also showed that increasing concrete strength did not lead to a linear increase in strength. The companion paper to this discusses differences in failure mode between heavily-reinforced specimens and lightly-reinforced specimens which fail at different steel yield strains.

Keywords: reinforced concrete; shear; size effect; two-way shear



1. Introduction

Size effect is a phenomenon in which the observed unit shear strength of reinforced concrete elements loaded in one-way shear decreases with increasing depth. The subject has been the topic of repeated investigation since the 1960s and has recently been incorporated into ACI 318-19 “Building Code Requirements for Structural Concrete” [1]. An illustration of how this phenomenon was incorporated into ACI 318-19 for one-way shear is shown in Fig.1. The corresponding equation is shown in Eq. (1) below:

$$\lambda_s = \sqrt{\frac{2}{1+d/10}} \quad (1)$$

where λ_s is the size effect factor, and d is the effective depth in inches. For metric, d is in millimeters and the 10 in the denominator becomes 250. This expression would suggest a reduction in unit shear strength of approximately 36% as effective depth increases from 250mm to 1000mm.

The strength of pile caps is often calculated using strut-and-tie models due to their geometry and loading conditions, which do not lend themselves to conventional flexural analyses. In the past, researchers have focused on comparing the ability of strut-and-tie models to estimate the strength of pile caps, and have gone on to propose bearing stress as the best estimate of “shear strength” of pile caps [2]. More recently, researchers have focused on the influence of shear span ratio and the effect of secondary reinforcement [3]. But there remains to be a systematic study of the effect of size on unit shear strength. The present investigation studies whether such an effect is present for deep reinforced concrete pile caps loaded in two-way shear. This study addresses this gap through the testing and analysis of twelve deep reinforced concrete pile caps across three scales, as shown in Fig.2. This paper is the first of a two-part series, the companion of which discusses the effect of reinforcement strain on failure.

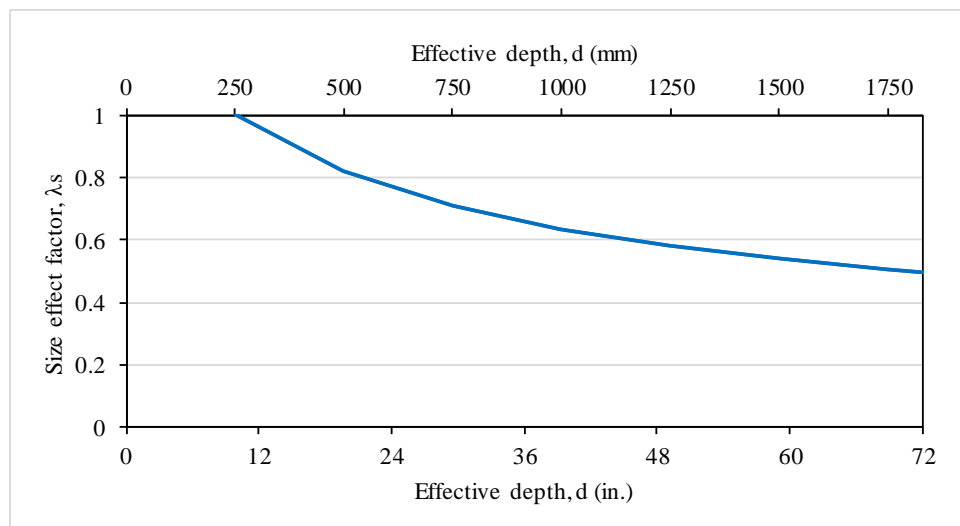


Fig. 1 – Size effect factor for one-way shear in ACI 318-19.

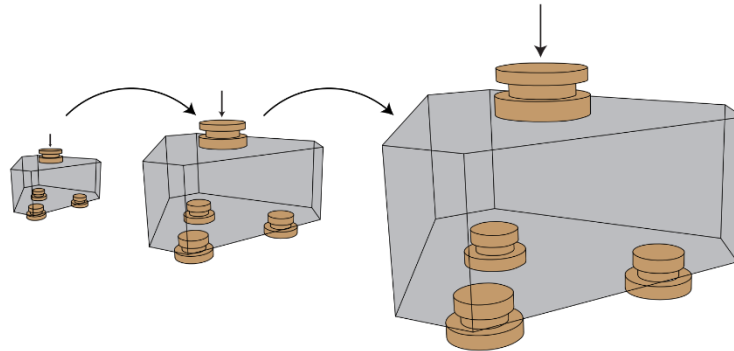


Fig. 2 – Specimen scales: S, M, and L.

2. Experiment Program

2.1 Specimens

Twelve specimens were built and tested. A summary of specimen properties is shown in Table 1. The dimensions of the specimens were all scaled from the largest specimen, which had an effective depth of $d=1000\text{mm}$ and a shear span ratio of $a=1000\text{mm}$ (as measured from the center of the upper surface to the centroid of steel above the lower bearing plate). From this “L-size” specimen, M-size specimen dimensions were halved ($a=d=500\text{mm}$), and S-size specimens were halved again ($a=d=250\text{mm}$). Fig.2 illustrates the sizes of the specimens relative to one another. In all specimens, the same concrete mix proportions were used, with a maximum aggregate size of 10mm. In eleven of twelve specimens, the concrete mix had a target compressive strength of $f'_c = 40\text{ MPa}$. In the remaining specimen (L3H), the target compressive strength of the concrete was $f'_c = 60\text{ MPa}$.

Two types of specimens were tested. In one type, the longitudinal steel reinforcement was proportioned with the goal of inducing a shear failure prior to steel yielding. To achieve this, three layers of five high-strength D38 deformed bars were used along each lower span of the L-size specimens. The resulting flexural reinforcement ratio was approximately 1.7%. Details of the geometry and reinforcement for this specimen are shown in Fig.3. In the M-size and S-size specimens, the bar diameter was reduced to D19 and D10, respectively and the geometry was halved and quartered, respectively. Fig.4 shows an example of the reinforcing cage and formwork for a single M-size specimen. A second type of specimen (lightly-reinforced) was also tested in which a single layer of five bars was used along each lower span, for a flexural reinforcement ratio of approximately 0.6%. None of the specimens had shear reinforcement.

The specimens were assigned alphanumeric names based on their size, number of layers of reinforcement, and concrete strength as follows:

- a. Size: L=large, M=medium, S=small, as described before
- b. Number of layers of reinforcement (1 or 3)
- c. Indicates tests of duplicate specimens (a, b, c) or if high-strength concrete was used (H).

For example, L3a and L3b denote duplicate L-size specimens with three layers of reinforcement, and L3H denotes the single L-size specimen with high-strength concrete and three layers of reinforcement.



Table 1 – Summary of concrete strength and test results.

Specimen	a = d, mm	Average f'_c (cores), MPa	Cast cores average f'_c , MPa	Strength P_u , kN	$\sigma_u = P_u/A_{top}$, MPa
L3H	1000	58.6	58.6	26,580	52.9
L3a		37.2	37.2	21,060	41.9
L3b		43.9	43.9	23,420	46.6
L1		44.9	44.9	16,510	32.9
M3a	500	45.1	43.2	5,710	45.4
M3b		39.6		6,110	48.6
M3c		48.9		5,810	46.2
M1		43.4		3,820	30.4
S3a	250	43.0		1,680	53.4
S3b		41.9		1,740	55.4
S3c		41.8		1,580	50.3
S1		41.5		1,210	38.5

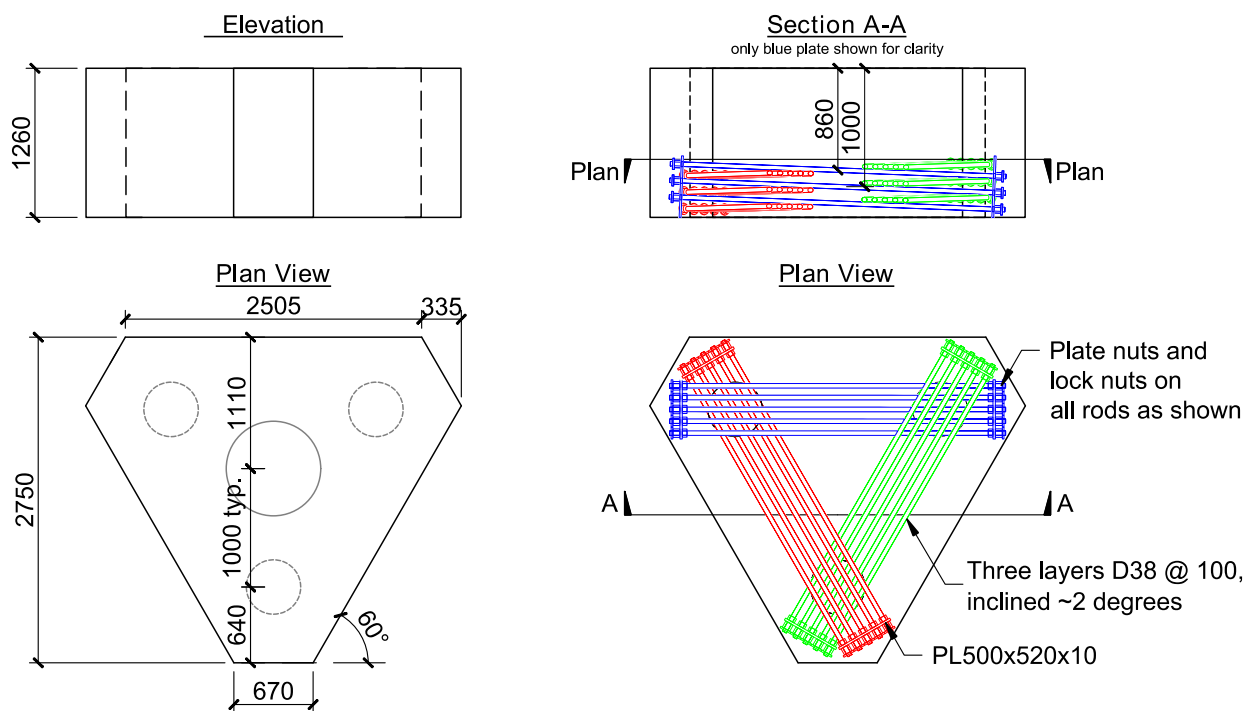


Fig. 3 – Details of reinforcement for largest specimen.



Fig. 4 – Photograph of formwork, reinforcement, and anchors for medium specimen.

2.2 Setup & Instrumentation

The specimens were tested under unidirectional loading to failure in the Bi-Axial dynamic Testing System (BATS) at the National Center for Research on Earthquake Engineering in Tainan, Taiwan. Before testing, bearing plates were installed on the upper and lower surfaces, with a thin layer of gypsum cement between the plate and specimen surface to provide uniform contact. Between these plates and the testing machine, spherical bearings were installed to allow the supports to move freely. Below the lower bearing-plate assemblies, acetal sheets also were installed in order to allow the lower bearing plates to spread laterally with minimal resistance.

The specimens were instrumented using strain gages, displacement meters, and digital cameras. Strain gages were installed at midspan of selected lower reinforcing bars to obtain a representative sample of the various bar locations, as shown in Fig.5.

The layout of displacement meters evolved as the testing program progressed. At the beginning of the testing program, displacement meters were arranged to measure vertical displacements of the lower surface of the specimen below the center and at midspan between the lower supports. As the test series progressed, additional meters were added to measure localized vertical deformations around bearing plates, horizontal movements of the narrower vertical faces, and vertical elongation along the longer vertical faces. Fig.6 shows meters for one of the largest-size specimens. Vertical meters were attached to an instrumentation truss which hung from bolts embedded on the narrower side surfaces of the specimens. The reason for attaching meters to a hanging truss was to avoid introducing measurement error due to seating losses of the bearings or relative movements between an external instrumentation truss and the specimen.

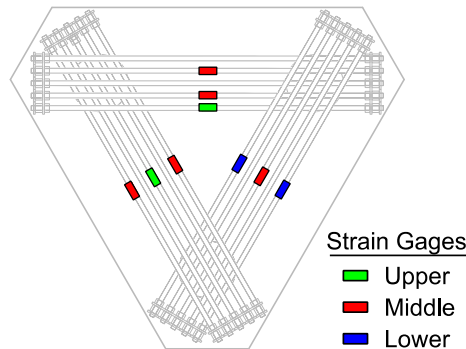


Fig. 5 – Strain gage layout.

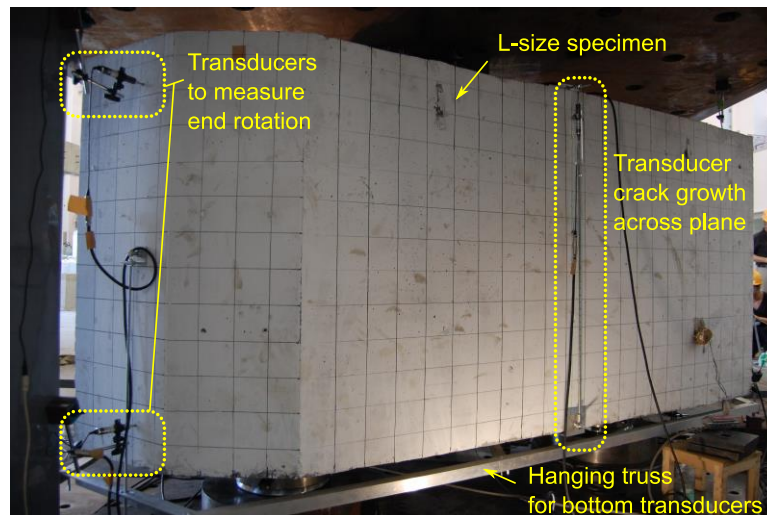


Fig. 6 – Overview of side displacement meters on L-size specimen.

3. Results & Discussion

This section presents and discusses general results from the experimental program, including a discussion of the overall force-displacement response and the effect of size on strength for specimens with three layers of reinforcement. More detailed discussion of the strain and displacement behavior is found in the Part 2 companion paper. To facilitate discussion, peak strengths reached by all specimens are summarized in Table 1 alongside concrete core test results.

3.1 Behavior

Two specimens with similar concrete compressive strengths at different size extremes were selected to compare the overall force-displacement response. Fig.7 shows a plot of force versus displacement for these specimens. To facilitate comparison, the range of the vertical force axis for S3a was scaled down by a factor of $(1/4)^2$, and the range of the horizontal axis (downward displacement) was scaled down by a factor of $(1/2)^2$. The two specimens show remarkably similar initial stiffness until approximately 9,500 kN (L3b axis), but the larger specimen reached a relatively smaller peak load. After the point at apparent cracking, the larger specimen also experienced a larger reduction in stiffness. After reaching its peak, the larger specimen also exhibited a more rapid reduction in resistance with increasing displacement demand.

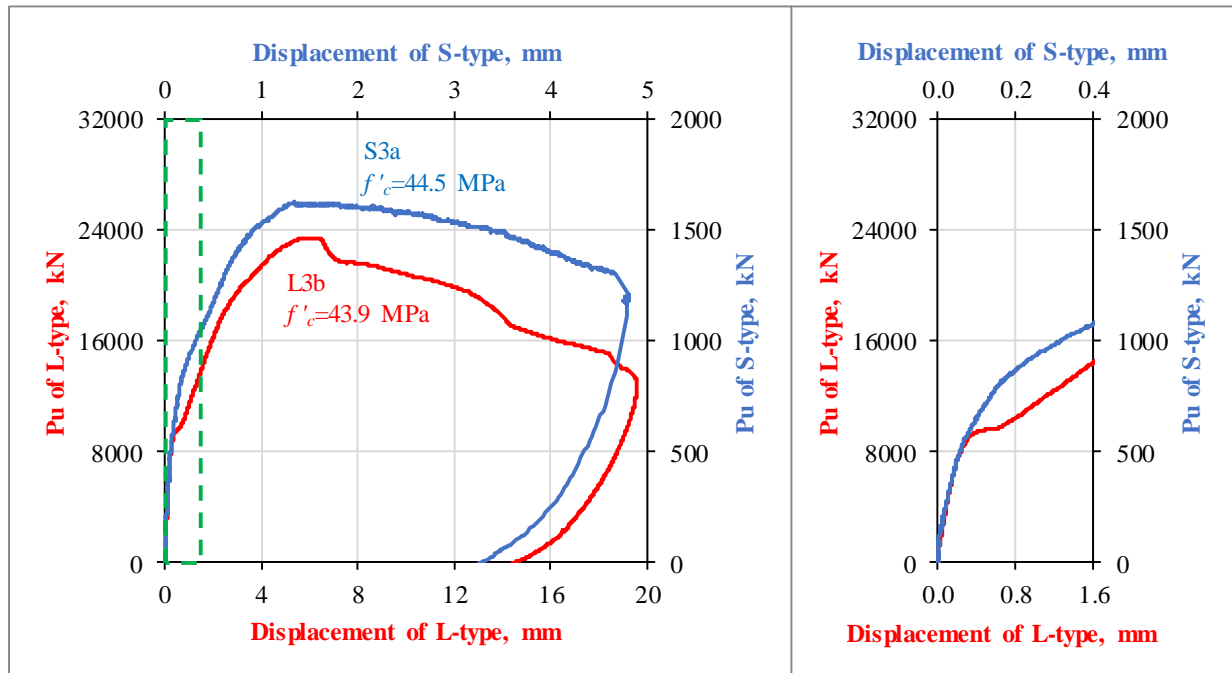


Fig. 7 – Comparison of curves for S3a and L3b: (left) overall view, and (right) close-up view as indicated in the green dashed square on the left.

3.2 Strength

Specimen strengths are summarized in Table 1. To facilitate comparison, these strengths were first normalized by the top bearing area, A_{top} , to obtain bearing strength, σ_u . This bearing strength is plotted against group mean concrete core strength in Fig.8 for specimens with three layers of reinforcement. Group mean concrete core strength was used because the specimens were cast from multiple batches of concrete that reached different compressive strengths. Each L-size specimen was cast from a single batch of concrete, and all M- and S-size specimens were cast from a single batch, which is why all M- and S-size specimens lie along the same vertical line in Fig.8.

The results from L-series tests shown in Fig.8 also indicate that increasing concrete strength did not lead to a corresponding linear increase in bearing strength. For instance, when concrete compressive strength increased by 35% from 43.9 MPa (as in L3b) to 58.6 MPa (as in L3H), bearing strength increased by just 13%. Similarly, comparing L3a to L3H, increasing concrete compressive strength by 57% led to just a 26% increase in specimen strength. These observations suggest that, to compare test results from specimens with different concrete strengths, bearing strength should not be normalized by compressive strength, but some factor of compressive strength. In the U.S., concrete compressive strength has historically been related to shear strength using a square root factor. This factor appears to fit the data well. If one considers L3a and L3H, $\sqrt{1.57}=1.25$, which is close to the 26% increase in strength observed. Similarly, considering L3b and L3H, $\sqrt{1.35}=1.16$, which is close to the 13% increase in strength observed. Following this logic, the bearing strength of each specimen was normalized by a factor consisting of the ratio of $\sqrt{40 \text{ MPa}}$ (considering the target strength) to the square root of the group mean core compressive strength:

$$\sigma_{u,norm} = \frac{\sqrt{40}}{\sqrt{f'_{c,group}}} \quad (2)$$



The process Eq. (2) can be seen graphically in the plot on the right in Fig.8. Compared with the left plot, the x-axis has changed from $f'_{c,group}$ to $\sqrt{f'_{c,group}}$. The filled points in the right plot represent values that have not yet been normalized. Eq. (2) projects these points towards the origin and determines their intersection with the dashed gray, vertical line, which denotes $\sqrt{40 \text{ MPa}}$. The normalized values are shown as unfilled points. For example, for S3a: $\sqrt{40}/\sqrt{43.2} \times 53.4 \text{ MPa} = 0.96 \times 53.4 \text{ MPa} = 51.4 \text{ MPa}$.

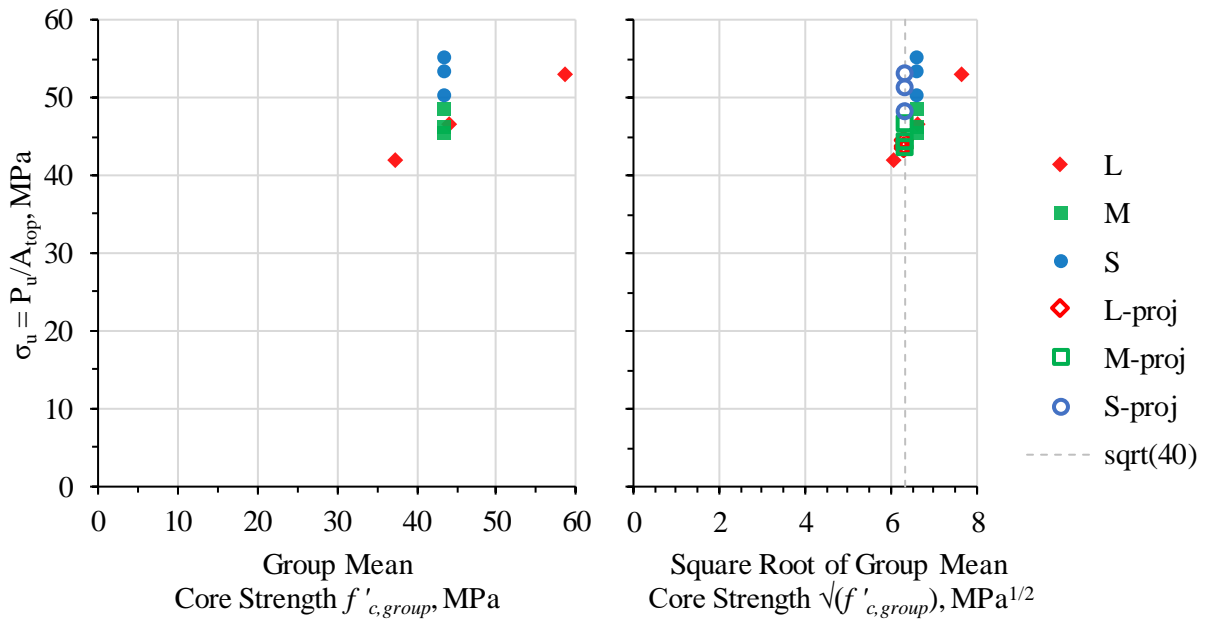


Fig. 8 – Bearing strengths of specimens with three layers of reinforcement (left) versus group mean core compressive strength, and (right) versus the square root of group mean core strength.

With strength now normalized to bearing area and concrete compressive strength, size effect may be examined. Fig.9 shows a plot of normalized bearing strength versus effective depth, again for specimens with three layers of bottom reinforcement. Overall, there is a trend of decreasing strength with increasing effective depth, but this trend is much less dramatic than what would be expected from the ACI 318-19 size effect factor for one-way shear in Fig.1. M-sized specimens ($d=500\text{mm}$) were on average 12% weaker than S-sized specimens ($d=250\text{mm}$), compared with 18% from the ACI 318-19 one-way shear methodology. Similarly, L-sized specimens ($d=1000\text{mm}$) were on average 14% weaker than S-sized specimens ($d=250\text{mm}$), compared with 36%. These results suggest that the diminishing reduction approach employed by ACI 318-19 for one-way shear is appropriate, but the magnitude of the reduction may not be as severe for specimens loaded in two-way shear as for specimens loaded in one-way shear.

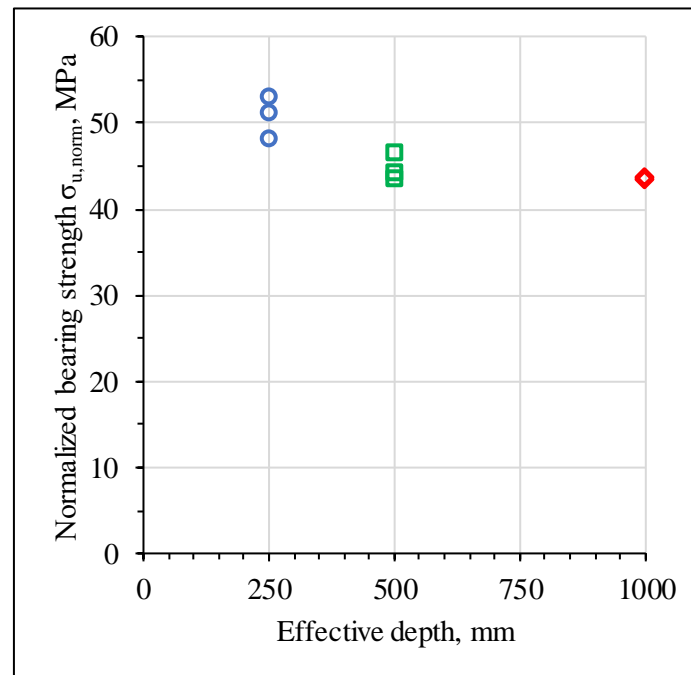


Fig. 9 – Normalized bearing strength versus effective depth for specimens with three layers of reinforcement.

4. Conclusions

This investigation was motivated by reported observations of a decrease in unit shear strength of deep beams loaded in one-way shear when compared with shallower counterparts. This phenomenon has been dubbed the “size effect” and has been incorporated into building codes around the world. The goal of this investigation was to study the “size effect” for pile cap specimens loaded in two-way shear. Experiments were conducted on twelve triangular pile caps with effective depths of 250mm, 500mm, and 1000mm. The specimens were loaded under monotonically-increasing axial load until failure. Nine specimens had large ratios of longitudinal reinforcement with the goal of inducing shear failure prior to flexural deformation. The remaining three specimens had modest longitudinal reinforcement ratios, approximately one-third that of the prior nine specimens. This paper focuses on test results from the nine specimens with larger reinforcement ratios. Within the ranges of variables considered, the results indicate that there is a diminishing decrease in unit strength with increasing effective depth. For the specimens tested, as effective depth doubled from 250mm to 500mm, unit strength decreased by 12%. As effective depth doubled again, unit strength decreased by another 2%.

5. References

- [1] ACI 318 (2019), “Building Code Requirements for Structural Concrete.” American Concrete Institute, Farmington Hills, Michigan, USA.
- [2] Adebar P and Zhou L (1996), “Design of Deep Pile Caps by Strut-and-Tie Models.” American Concrete Institute Structural Journal, 93(4), 437-448.
- [3] Miguel-Tortola L, Pallares L, Francisco Miguel P (2018), “Punching shear failure in three-pile caps: Influence of the shear span-depth ratio and secondary reinforcement.” Engineering Structures, Vol. 155, pp. 127-143.



6. Acknowledgments

This research was conducted using the fund of Kasai Laboratory supported by KYB, Showa Densen Cable System, Japan Steel Consortium, Bridgestone, and OILES corporations. The reinforcing bars and anchor devices were provided by Kyoiei-Seiko Corporation. Invaluable advice was given by the members of the committee headed by Professor Akira Wada. Professor Shyh-Jiann Hwang of NCREE, Taiwan, greatly contributed to this project. Dr. Srinivas Mogili of NCREE, Taiwan, supervised the cutting of the specimens.